



Long-term monitor on Mrk 421 TeV emission using ARGO-YBJ experiment

S.Z. CHEN¹, ON BEHALF OF THE ARGO-YBJ COLLABORATION

¹Particle & Astrophysics Center, Institute of High Energy Physics, CAS

chensz@ihep.ac.cn

Abstract: ARGO-YBJ is an air shower detector array with a fully covered layer of resistive plate chambers. It is operated with a high duty cycle and a large field of view. It continuously monitors the northern sky at energies above 0.3 TeV. In this paper, we report a long-term monitoring of Mrk 421 over the period from 2007 November to 2011 February, including both quiet and active phases. This source was observed by the satellite-borne experiments RXTE and Swift in the X-ray band. The γ -ray flux observed by ARGO-YBJ has a clear correlation with the X-ray flux. No lag longer than 1 day between the X-ray and γ -ray photons is found. The evolution of the spectral energy distribution is investigated by measuring spectral indices at four different flux levels. Hardening of the spectra is observed in both X-ray and γ -ray bands. The γ -ray flux increases quadratically with the simultaneously measured X-ray flux. All these observational results strongly favor the synchrotron self-Compton process as the underlying radiative mechanism.

Keywords: Mrk 421, gamma ray observation, AGN, ARGO-YBJ

1 Introduction

Mrk 421 ($z = 0.031$) is one of the brightest blazars known and is classified as a BL Lac object, a subclass of active galactic nuclei (AGNs). Its emission, like that of the other blazars, is generally dominated by nonthermal radiation from a relativistic jet aligned along our line of sight. The spectral energy distribution (SED) is double-humped at X-ray and γ -ray energies in a plot of νF_ν versus ν [1], where ν is the frequency and F_ν is the flux density. The hump at low energies is usually interpreted to be caused by synchrotron radiation from relativistic electrons (and positrons) within the jet. The origin of the hump at high energies is under debate. Many models attribute the high-energy emission to the inverse Compton scattering of the synchrotron (synchrotron self-Compton, SSC) or external photons (external Compton, EC) by the same population of relativistic electrons [2, 3], therefore a X-ray/ γ -ray correlation would be expected. Other models invoke hadronic processes including proton-initiated cascades and/or proton-synchrotron emission in a magnetic field-dominated jet.

Mrk 421 is a very active blazar with major outbursts about once every two years in both X-ray and γ -ray. A major outburst usually lasts several months and is accompanied by many rapid flares with timescales from tens of minutes to several days. Its high variability and broadband emission require long-term, well-sampled, multiwavelength observations in order to understand the emission mechanisms of these outbursts. A long-term simultaneous X-ray/ γ -ray observation is better performed by means of a combination of satellite-borne X-ray experiments and wide field-of-view

air shower experiments, such as the ARGO-YBJ experiment [4], which are operated day and night with a duty cycle higher than 86% and can observe any source with a zenith angle less than 50° . This is essential in investigating the temporal features of AGN emissions. The ARGO-YBJ experiment has been continuously monitoring the northern sky for outbursts from all AGNs such as Mrk 421 since 2006 July. Meanwhile, these sources were also monitored by the satellite-borne X-ray detectors ASM/RXTE and BAT/Swift. In this paper, we report on the long-term monitoring of Mrk 421 for γ -ray outbursts and on the correlation between γ -rays and simultaneous X-rays over the period from 2007 November to 2011 February.

2 The ARGO-YBJ experiment and Data analysis

The ARGO-YBJ experiment, located in Tibet, China at an altitude of 4300 m a.s.l., is the result of a collaboration among Chinese and Italian institutions and is designed for very high energy (VHE) γ -ray astronomy and cosmic ray observations. The detector consists of a single layer of resistive plate chambers (RPCs). One hundred thirty clusters (a cluster composed of 12 RPCs) are installed to form a carpet of about 5600 m² with an active area of $\sim 93\%$. This central carpet is surrounded by 23 additional clusters (a “guard ring”) to improve the reconstruction of the shower core location. The total area of the array is 110 m \times 100 m. More details about the detector and RPC performance can be found in [4, 5]. The high granularity of the appa-

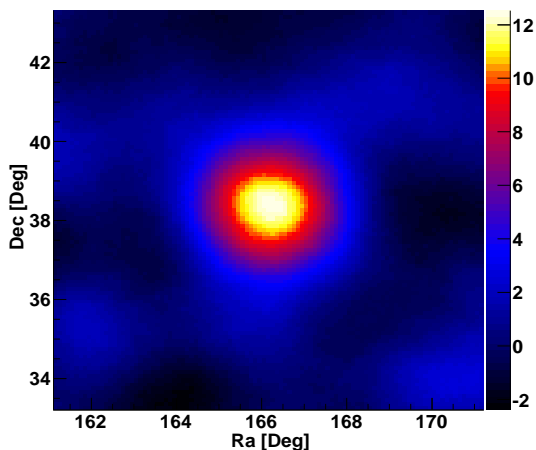


Figure 1: Distribution of statistical significance around Mrk 421.

ratus permits a detailed spatial-temporal reconstruction of the shower profile and therefore the incident direction of the primary particle. The arrival time of the particles is measured by Time to Digital Converters (TDCs) with a resolution of approximately 1.8 ns. This results in an angular resolution of 0.2 degree for showers with energy above 10 TeV and 2.5 degree at approximately 100 GeV. The central 130 clusters began taking data in 2006 July, and the “guard ring” was merged into the DAQ stream in 2007 November. The trigger rate is ~ 3.5 kHz with a dead time of 4% and the average duty cycle is higher than 86%.

To achieve a better angular resolution, the event selections used in [6] is applied here and only events with a zenith angle less than 50° are used. In order to obtain a sky map using events, an area centered at the source location in celestial coordinates (right ascension and declination) is divided into a grid of $0.1^\circ \times 0.1^\circ$ bins and filled with detected events according to their reconstructed origin. In order to extract an excess of γ -rays from the source, the so-called “direct integral method” [7] is adopted to estimate the number of cosmic ray background events in the bin. To remove the affection of large scale anisotropy, a correction has been applied which can be found in [6]. The Li-Ma formula [8] is used to estimate the significance.

3 Results

The data used in this paper were collected by the ARGO-YBJ experiment in the period from 2007 November to 2011 February. The total lifetime is 1024.0 days. The total number of events after being filtered is 1.7×10^{11} . A clear signal from Mrk 421 with significance greater than 12 standard deviations is observed using events with $N_{pad} > 60$ (see Figure 1). A signal at such a level of significance allows us to study flux variations, correlations with the X-ray flux, and the evolution of the SED.

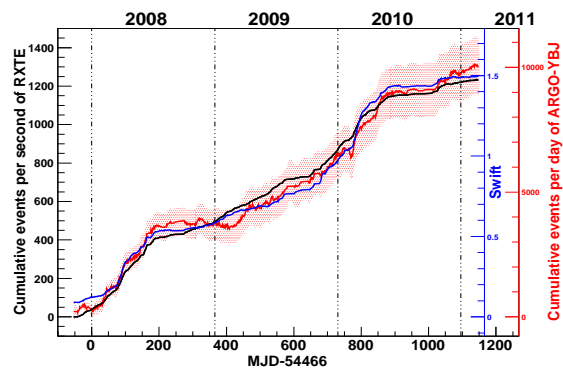


Figure 2: Cumulative light curves from the Mrk 421 direction: the red curve is the γ -ray result observed by ARGO-YBJ and the shaded red region indicates the corresponding 1σ statistical error; the black curve represents soft X-rays (2-12 keV) observed by ASM/RXTE; hard X-rays (15-50 keV) observed by BAT/Swift are given by the blue curve and the scale has been normalized to the ASM/RXTE one.

3.1 Temporal Analysis

In order to study the correlation between γ -rays and X-rays, the daily averaged light curves of both the hard X-rays (15-50 keV) measured by BAT/Swift¹ and the soft X-rays (2-12 keV) measured by ASM/RXTE² are used. The observations by RXTE and Swift have a rather long exposure by orbiting the Earth every 1.5 hr. No matter in day time or night time, ARGO-YBJ observes Mrk-421 while the AGN is within its field of view. A typical transit lasts usually 6 hr.

In 804 days all three experiments observed Mrk 421 simultaneously. In Figure 2 the accumulation of event rates from the Mrk 421 direction is shown. The ARGO-YBJ curve is obtained using events with $N_{pad} > 100$, thus the median energy of the observed photons is 1.8 TeV, assuming a spectral index is -2.4 . The rapid increase in the three curves indicates that the source had a long-term outburst at the beginning of 2008, which is a combination of several large flares (see [6] for details). The following quiet state lasted for about 200 days. Afterward Mrk 421 became increasingly active. In fact, there were flares in 2009 November [9]. The duty cycle of ARGO-YBJ was low due to detector maintenance, therefore it is not obvious in Figure 2. There was a large flare in 2010 February [9, 10], which can be also read from the rapid increase of the three curves in Figure 2. Details analysis about this large flare with multi-wavelength can be found in [11]. It can be concluded that there exists a good long-term correlation between γ -rays and X-rays.

The discrete correlation function (DCF) [13] is used to quantify the degree of correlation and the phase differ-

1. Transient monitor results provided by the BAT/Swift team: <http://heasarc.gsfc.nasa.gov/docs/swift/results/transients/weak/Mrk421/>.
2. Quick-look results provided by the ASM/RXTE team: http://xte.mit.edu/ASM_lc.html.

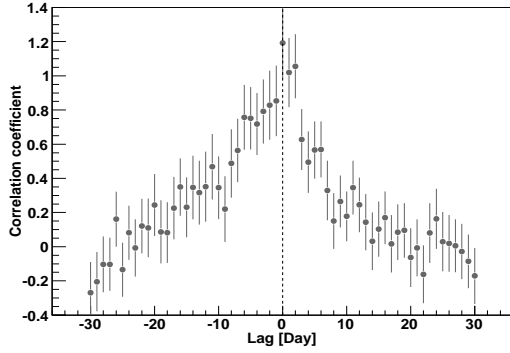


Figure 3: Discrete correlation function between X-ray (2–12 keV) and γ -ray light curves.

ences (lags) in the variations between γ -rays and X-rays. The daily fluxes are used for this analysis. The DCF (in 1 day bins) derived from RXTE and ARGO-YBJ data (with $N_{pad} > 100$) is shown in Figure 3, where a positive value means that γ -rays lag behind X-rays. The peak of the distribution is around zero. No significant lag longer than 1 day is found.

3.2 Spectral Energy Distribution

To study the SED at different flux levels, the data simultaneously observed in γ -ray and X-ray bands are divided into four groups according to the observational time periods in which the ASM/RXTE counting rate is 0–2, 2–3, 3–5 or >5 $\text{cm}^{-2} \text{s}^{-1}$. For each group, a flux-averaged SED is constructed both at γ -ray and X-ray energies.

ASM/RXTE monitors the X-ray emission from Mrk 421 at three energy bands, i.e. 1.5–3, 3–5 and 5–12 keV [14]. In the flux estimation, the hydrogen column density $1.38 \times 10^{20} \text{cm}^{-2}$ [15] and a power law spectrum are assumed. The best-fit spectral indices for the four flux levels are -2.38 ± 0.04 , -2.09 ± 0.03 , -2.03 ± 0.03 and -2.00 ± 0.08 , respectively, in which only statistical errors are taken into account. This result is shown in Figure 4 which is consistent with the analysis of [16] where a spectral hardening towards high fluxes is also reported based on a shorter timescale observation. This indicates that this correlation is independent of the timescale.

To estimate the spectrum of γ -rays with a distribution of the number of events in excess as a function of N_{pad} , we apply the method used in [6]. The resulting spectrum from the direction of the Crab Nebula is $(3.98 \pm 0.28_{stat}) \times 10^{-11} (\text{E}/\text{TeV})^{-2.61 \pm 0.08_{stat}}$ photons $\text{TeV}^{-1} \text{cm}^{-2} \text{s}^{-1}$, which is in agreement with observations by other detectors [6]. By applying this procedure to Mrk421 we obtain the spectra for the four event groups with different flux levels. To remove the influence caused by absorption of γ -rays in the extragalactic background light, we adopt the optical depth estimated by Franceschini [17]. The spectral indices in the energy range from 300 GeV to 10

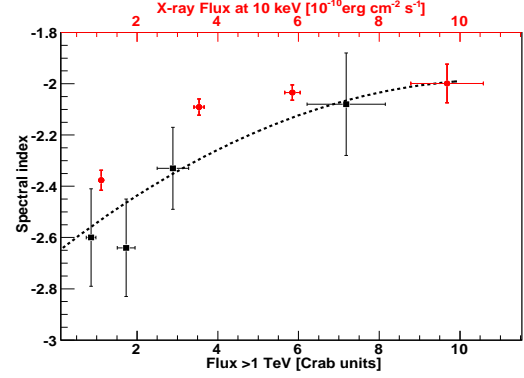


Figure 4: Red: Correlation between the X-ray flux at 10 keV and the corresponding photon index at 2–12 keV. Black: Spectral index vs. γ -ray flux above 1 TeV. The dashed line is the function obtained by the Whipple experiment [18].

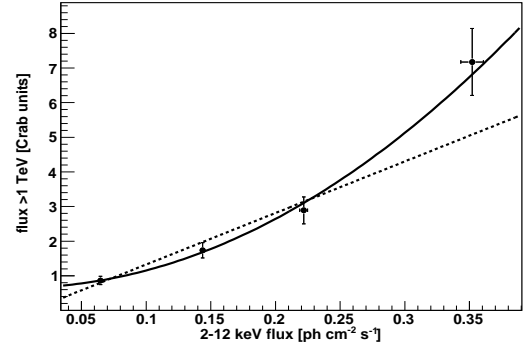


Figure 5: γ -ray flux above 1 TeV vs. X-ray flux at 2–12 keV. The solid line is a quadratic fit using function $y = ax^2 + b$ which yields $\chi^2/dof = 0.47/2$. The dotted line is a linear fit which yields $\chi^2/dof = 6.45/2$, where dof refers to degrees of freedom.

TeV are -2.60 ± 0.19 , -2.64 ± 0.19 , -2.33 ± 0.16 and -2.08 ± 0.20 , respectively. Only statistical error is quoted. The corresponding flux above 1 TeV ranges from 0.8 to 7 times that of the Crab Nebula unit, i.e. 2.47×10^{-11} photons $\text{cm}^{-2} \text{s}^{-1}$. The spectra seem to become harder with the increase of flux, as indicated in Figure 4, in agreement with the function obtained by the Whipple experiment [18]. The quoted errors in Figure 4 are statistical. The systematic error is estimated to be $\leq 30\%$ in the flux level determination [12].

Using the spectra described above, we investigate the correlation between γ -ray and X-ray fluxes. Figure 5 shows the integral γ -ray flux above 1 TeV as a function of the integral X-ray flux from 2 keV to 12 keV: a positive correlation is observed. A quadratic fit (with the function $y = ax^2 + b$) to the data points yields $\chi^2/dof = 0.47/2$, while a linear fit yields $\chi^2/dof = 6.45/2$, where dof refers to degrees of freedom. The observation favors a quadratic correlation between γ -ray and X-ray fluxes. A similar quadratic cor-

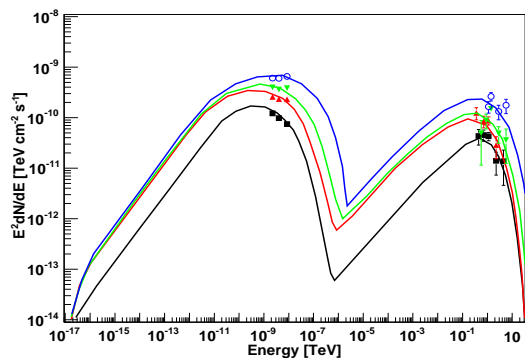


Figure 6: Spectral energy distribution of Mrk 421 derived from 4 flux level data groups. The solid line shows the best fit to the data with an homogeneous one-zone SSC model. The curves from low to high are in black, red, green and blue.

relation has been reported by [19]. In contrast, an observation with linear correlation is obtained by [20]. According to [21], changes of the magnetic field, electron density and adiabatic cooling may be associated with different correlations between γ -ray and X-ray fluxes.

3.3 Modelling of the X-ray and γ -ray emissions

A fit to the four flux-averaged SEDs with an homogeneous one-zone SSC model proposed by [22] is performed. Details about the parameters and the fitting process could be found in [6]. The best fits are shown in Figure 6 for different flux levels, with the corresponding parameters given in Table 1.

4 Conclusion

Mrk 421 is a very active blazar with frequent outbursts, which are composed of many flares and can last as long as a few months. This makes this blazar an excellent candidate for the study of the jet physics in AGNs. A strong correlation between its γ -ray and X-ray emissions has been confirmed by many observations in the past decade (for a review see [23]). Most of the previous γ -ray observations, however, are carried out by Cherenkov telescopes with limited exposure, therefore, they usually focus on short timescales. On the contrary, the high duty cycle of the ARGO-YBJ experiment makes possible a long-term and continuous observation of this variable source, allowing a simultaneous monitoring of γ -rays and X-rays for about two years. That increases the set of long-term simultaneous multiwavelength observations of Mrk 421, which are essential for studying the correlation between energy bands where different emission mechanisms are at work.

In conclusion, we have presented a long-term continuous monitoring of Mrk 421 and a correlation between γ -rays observed by the ARGO-YBJ experiment and satellite-

Table 1: List of the best parameters in SSC model.

levels	1	2	3	4
γ_{max}	7×10^5	7×10^5	1×10^6	2×10^6
l_e	6×10^{-6}	1×10^{-5}	1×10^{-5}	1.4×10^{-5}
B (G)	0.08	0.15	0.15	0.15
R (cm)	5×10^{16}	5×10^{16}	5×10^{16}	5×10^{16}
δ	16	15	15	15
α	1.7	1.7	1.7	1.7

borne X-ray data. The temporal and spectral analysis strongly support the predictions of the SSC model.

5 acknowledgments

This work is supported in China by NSFC (No.10120130794), the Chinese Ministry of Science and Technology, the Chinese Academy of Sciences, the Key Laboratory of Particle Astrophysics, CAS, and in Italy by the Istituto Nazionale di Fisica Nucleare (INFN).

We also acknowledge the essential supports of W.Y. Chen, G. Yang, X.F. Yuan, C.Y. Zhao, R. Assiro, B. Biondo, S. Bricola, F. Budano, A. Corvaglia, B. D'Aquino, R. Esposito, A. Innocente, A. Mangano, E. Pastori, C. Pinto, E. Reali, F. Taurino and A. Zerbini, in the installation, debugging and maintenance of the detector.

References

- [1] Fossati, G., et al. 1998, MNRAS, 299, 433
- [2] Ghisellini, G., et al. 1998, MNRAS, 301, 451
- [3] Dermer, C. D., et al. 1992, A&A, 256, L27
- [4] Aielli, G., et al. 2006, Nucl. Instrum. Meth. A, 562, 92
- [5] Aielli, G., et al. 2009, Nucl. Instrum. Meth. A, 608, 246
- [6] Bartoli, B., et al. 2011, ApJ, 734, 110, or arXiv:1106.0896v1
- [7] Fleysher, R., et al. 2004, ApJ, 603, 355
- [8] Li, T.P., & Ma, Y.Q. 1983, ApJ, 272, 317
- [9] Isobe, N., et al. 2010, PASJ, 62, L55
- [10] Ong, R.A., 2010, ATel#2443
- [11] Chen, S.Z., 2011, 32nd ICRC, NO.1209
- [12] Aielli, G., et al. 2010, ApJ, 714, L208
- [13] Edelson, R.R., & Krolik, J.H. 1988, ApJ, 333, 646
- [14] Levine, A. M., et al. 1996, ApJ, 467, L33
- [15] Dickey, J., Lockman, J. 1990, ARA&A, 28, 215
- [16] Rebillot, P.F., et al. 2006, ApJ, 641, 740
- [17] Franceschini, A., et al. 2008, A&A, 487, 837
- [18] Krennrich, F., et al. 2002, ApJ, 575, L9
- [19] Fossati, G., et al. 2008, ApJ, 677, 906
- [20] Amenomori, M., et al. 2003, ApJ, 598, 242
- [21] Katarzyński, K., et al. 2005, A&A, 433, 479
- [22] Mastichiadis, A. & Kirk, J.G. 1995, ApJ, 295, 613
- [23] Wagner, R., 2008, arXiv:0808.2483v1.